Ross Sukunya (Orcid ID: 0000-0001-5593-6779)

Multifunctional core-shell electrospun nanofibrous fabrics of poly(vinyl alcohol)/silk sericin (core) and poly(lactide-*co*-glycolide) (shell)

Nantaprapa Tuancharoensri[a], Gareth Ross[a,b], Winita Punyodom[c,d], Sararat Mahasaranon[a,b], Jirapas Jongjitwimol[e], Paul D Topham[f], Sukunya Ross[a,b,*]

[a]Department of Chemistry, Faculty of Science, Naresuan University, Phitsanulok 65000, Thailand

[b]Biopolymer Group, Excellent Center of Biomaterials, Department of Chemistry, Faculty of Science, Naresuan University, Phitsanulok 65000, Thailand

[c]Center of Excellence in Materials Science and Technology, Chiang Mai University, Chiang Mai, 50200, Thailand

[d] Department of Chemistry, Faculty of Science, Chiang Mai University, Chiang Mai, 50200, Thailand

[e]Clinical Microbiology, Department of Medical Technology, Faculty of Allied Health Sciences, Naresuan University, Phitsanulok, Thailand

[f]Aston Institute of Materials Research, Aston University, Birmingham, UK

Phone +6655 963 445, Fax. +6655 963 402, [*]e-mail: sukunyaj@nu.ac.th

Abstract

Core-shell fibres (CSFs) offer a simple route to multifunctional hybrid materials for a wide range of applications. Herein, we report the design of a core-shell electrospun nanofibrous fabric containing a hydrophilic core and hydrophobic shell. CSFs were fabricated for the first time from poly(vinyl alcohol) (PVA)/silk sericin (SS from silk cocoons) as the core and poly(lactide-*co*-glycolide) (PLGA) as the shell. The core serves as a potential carrier for water-soluble bioactive agents, and the shell works as a barrier to prevent premature release of water-soluble agents from the core. The effect of molecular weight of PLGA and loading of SS on the morphology of fibers were studied. The parameters that significantly influence the core-shell electrospinning process were studied to elucidate the most effective conditions to create our multifunctional nanofibrous fabrics with smooth fiber morphology (diameters in the range 800-1300 nm) and low bead formation. Our CSFs were shown to degrade in saline buffer solution (pH 7.4) and were readily rendered with anti-bacterial properties against *S.aureus* and *E. coli* by post-spinning deposition of silver nanoparticles (AgNPs, 40 nm diameter) or

This article has been accepted for publication and undergone full peer review but has not been through the copyediting, typesetting, pagination and proofreading process which may lead to differences between this version and the Version of Record. Please cite this article as doi: 10.1002/pi.6319

cinnamon essential oil (CEO). The fibers were nontoxic to normal human dermal fibroblast cell lines, as the cells were shown to attach and proliferate on CSFs, CSF/AgNPs and CSF/CEO, with good cell tolerance for 72 hours of incubation. These smart multifunctional CSF show great potential towards smart delivery fabrics/dressings capable of carrying water-soluble bioactive agents surrounded by a protective, but degradable, antibacterial shell to guard the cargo for more effective controlled release.

Keywords: Electrospun nanofibers; Silk sericin; Poly(vinyl alcohol); Poly(lactide-*co*-glycolide); Core-shell structure

1. Introduction

Nanofibers are of great interest in an ever-increasing number of applications. They have widespread use in water and air filtration, spanning from industrial (car filters and water filters) to personal (facial masks) products, energy storage and biomedical applications. Due to their small diameter, nanofibers form highly porous structures with a large surface area-to-volume ratio. In addition to increased activity or function, this key feature enables nanofibrous structures to be used as an effective artificial extracellular matrix (ECM) for cell migration and growth.[1] Electrospinning is commonly used to fabricate nanofibrous fabrics due to its simplicity and productivity.[2-5] This technique allows for careful design and manipulation of the final properties of the nanofibers. For example, various active substances, such as magnetic nanoparticles, drugs, vitamins, growth factors and anti-bacterial agents, can be either added to the polymer solution before spinning or coated onto the fibers post-spinning.[6-11]

Several synthetic and natural polymers have been used as biomaterials for medical applications in the form of different structures, such as films, porous scaffolds and nanofibers, due to their biocompatibility and non-toxicity.[12-16] For electrospun nanofibers, promising materials include poly(lactic acid) (PLA),[4,16-18] poly(lactide-*co*-glycolide) (PLGA),[19-24] polycaprolactone (PCL),[4,25] poly(vinyl alcohol) (PVA),[3,26,27] poly(glycidyl methacrylate) (PGMA),[28-30] silk sericin (SS),[3,27,31,32] silk fibroin[33] and chitosan (CS).[17] For example, PLGA and silk fibroin hybrid scaffolds have been optimally fabricated for wound dressings and the *in vitro* results showed that the attachment and proliferation of mouse fibroblasts significantly increased on the PLGA/silk fibroin (2:1) scaffolds.[33] Core-shell composite nanofibers with a chitosan shell and PLA core were successfully fabricated with antibacterial efficiency of 100% for bacterial (*E.coli*) concentrations of 10^3 CFU/mL.[17] In a further example, Sedghi and Shaabani fabricated a CS core with PVA shell and added curcumin (a natural antimicrobial

activity) to the nanofibers to deliver protection against MRSA, *S. epidermidis*, *E.coli and P. aeruginosa*.[26]

The majority of the research is designed either with a hydrophilic or hydrophobic shell but with a hydrophobic core, mainly due to the difficulty in fabricating hydrophilic core with a hydrophobic shell.[26,34-36] The fabrication of core-shell nanofibers with a hydrophilic core requires precise control of the electrospinning parameters. For example, one difficulty arises from the differences in polymer solution parameters associated with the core and shell, especially when water is used as the spinning solvent for the core.

In this work, we have designed a new core-shell nanofiber with hydrophilic core and hydrophobic shell. For the first time, core-shell electrospun nanofibers comprising PVA/SS (hydrophilic core) and PLGA (hydrophobic shell) have been fabricated. The core layer serves as a carrier for water-soluble bioactive agents, growth factors and other agents, while the shell layer works as a barrier to prevent the premature release of these water-soluble agents from core component. Electrospinning parameters for the individual core, shell and combined core-shell have been carefully studied and optimum conditions identified. The core-shell morphology was confirmed by scanning electron microscope and transmission electron microscope. Furthermore, the antibacterial properties, *in vitro* cytotoxicity, cell proliferation, *in vitro* degradation and swelling ratio of our new smart nanofibrous meshes were evaluated for their potential use in future biomedical applications.

2. Experimental

2.1 Materials

PLGA (poly(lactic-*co*-glycolic acid)) with 75:25 LA:GA was supplied by the Bioplastic Production Laboratory for Medical Applications, Chiang Mai University. High molecular weight (HMW-PGLA, M_w = 108,000 g.mol^{-1}) and low molecular weight (LMW-PGLA, M_w = 20,000 g.mol^{-1}) copolymers were used. Chloroform and dimethylformamide (DMF) were purchased from RCI Labscan Limited, Bangkok, Thailand. Poly(vinyl alcohol) (PVA) was obtained from Sigma-Aldrich Co. Inc, Singapore (M_w = 85,000-124,000 g.mol^{-1}). Silk sericin (SS) was prepared by a water degumming process from silk cocoons (*Bombyx mori*) obtained from the Tak province in the lower northern region of Thailand. Silver nanoparticles (AgNP) were purchased from Sigma-Aldrich Co. Inc, USA (40 nm, 0.02 mg/mL). Cinnamon essential oil (CEO) was provided by SenOdos, GVI Life Care Co., Ltd., Bangkok, Thailand. For cell culture studies, normal human dermal fibroblasts cell lines (NHDF, Lot no.C-12302, Promocell, Eppelheim, Germany) cell line was provided by the Faculty of Pharmacy, Naresuan

University, Thailand. Dulbecco's Modified Eagle Medium (DMEM), Fetal bovine serum (FBS), Penicillin-streptomycin (Pen Strep), Amphotericin B and 0.25% Trypsin-EDTA were purchased from Gibco (Grand Island, NY, USA). XTT solution (Cell Proliferation Kit II) was supplied by Roche (Roche Diagnostics GmbH, Mannheim, Germany). Phosphate Buffer Silene (PBS) with pH 7.4 were supplied by KEMAUS, Australia.

2.2 Preparation of silk sericin powder using water degumming process

A simple organic solvent-free process of degumming was used to prepare the silk sericin powder.[37] Briefly, 20 g of silk cocoons were cut into small pieces and then boiled in 500 mL of DI water for 4 hrs. After the degumming process, the SS solution was dried into a powder in an oven at 75°C for 13–15 hours, and then kept in a desiccator for further use.

2.3 Fabrication of core, shell, and core-shell nanofibers

Core: PVA was dissolved in DI water (7% w/v) at 100 °C for 4 hrs. Different SS solutions (0, 1, 2 and 3 % w/v) were prepared by dissolving SS powder in DI water at 100 °C for 2 hrs. Appropriate PVA/SS solutions were mixed and fabricated into nanofibers by electrospinning using the conditions shown in Fig.1a. The spinning solutions were heated to 70 °C during the process.[3]

Shell: A 10% w/v solution of PLGA (75:25 LA:GA) was prepared by dissolving PLGA in a solvent mixture of 4:1 v/v chloroform and DMF to enhance the conductivity for electrospinning. The optimal processing conditions for electrospinning were as follows: 0.3 mL/h flow rate, 25 kV and a tip-to-collector distance of 15 cm.

Core-Shell: Core-shell electrospun nanofibers were fabricated using coaxial electrospinning where a spinneret composed of two coaxial needles were connected to separate high voltage power supplies. Two different polymer solutions were used, one for the core (hydrophilic PVA/SS) and one for the shell (hydrophobic PLGA); these were independently fed through the inner and outer needles, respectively. The coaxial needle had an inner diameter of 0.7 mm (22G) and outside needle gauge of 1.2 mm (18G). The optimal processing conditions for coaxial electrospinning were adjusted and were the same conditions used for electrospinning the core and shell described above. The core-shell electrospun nanofibers were collected on an aluminum foil collector and dried at room temperature.

2.4 Characterization

Morphology: The morphologies of the core, shell and core-shell electrospun nanofibers were observed using scanning electron microscopy (SEM, Leo model 1455VP) at 20 kV in

high vacuum. Samples were cut into squares of 0.5 x 0.5 mm and then mounted onto metal stubs before coating with gold to enhance electric conductivity. Transmission electron microscopy (TEM, TECNAI12 PHILIPS model) was used to determine the core-shell structure of electrospun nanofibers. Samples for TEM observation were directly spun onto a carbon-coated copper grid.

Chemical Functionality: The chemical functionality of the core, shell and core-shell electrospun nanofibers were confirmed using attenuated total reflection Fourier transform infrared (ATR-FTIR) spectroscopy with a PerkinElmer Spectrum GX (400–4000 cm^{-1}).

Hydrophilicity: Hydrophilic properties of the core, shell and core-shell electrospun nanofibers was measured by contact angle (CA, Dataphysics Model OCA20) at room temperature. Water was loaded into a syringe and 5.000 μL of drop volume with a 0.50 μL/s dispensing rate (slow) was used. Images of water droplets were recorded by HD camera and the contact angles of samples were measured (n = 6).

Crystallinity: Crystallinity of the core, shell and core-shell electrospun nanofibers was investigated by X-ray diffraction (XRD, Philips Model X'Pert Por) with a diffraction angle range (2θ) from 5 to 80 degrees (Cu K_{α}, 1.54 Å).

In-vitro degradation: The electrospun nanofiber samples were cut into square pieces (1 cm x 1 cm x 1 mm) and immersed in PBS solution (pH 7.4) at 37 ºC for 7, 21, 42 and 63 days. Separate samples were used for each degradation time period. At the end of each time period, the sample was removed from PBS and washed with DI water 3 times before vacuum drying for 24 hrs. The percentage weight loss was calculated by Eq. 1.

$$\%\, weight\ loss\ = \frac{w_i - w_d}{w_i} \text{x}100 \qquad \text{Eq. 1}$$

where w_i and w_d are the initial and dry weight, respectively.

Antibacterial activity: Silver nanoparticles (AgNPs) and cinnamon essential oil (CEO) were each assessed for their antibacterial activity by post-spinning deposition onto the core-shell electrospun nanofibers, this was achieved by spraying aqueous solutions of 0.4 mL of AgNPs (0.02 mg/mL) and 1 mL of 15 %v/v CEO in ethanol (0.15 mL CEO), respectively. The antibacterial activity of these nanofibers was evaluated against Gram-negative *E. coli* (ATCC 25922) and Gram-positive *S. aureus* (ATCC 25923). Samples were cut into discs (6 mm diameter) and sterilized by ozone gas. Nanofiber discs and control drug (Gentamicin) samples were placed onto Muller Hinton agar plates that contained a bacteria suspension and incubated

at 37 ºC. The inhibition zones were measured after 18 hrs using Vernier calipers and the plates were photographed.

Indirect in vitro cytotoxicity: The cytotoxicity of the core-shell electrospun nanofibers was studied by XTT assay. Nanofiber samples were cut to a size of 1 cm x 1 cm x 1 mm before being immersed in 1 mL of DMEM medium with serum-free at room temperature for 24 hrs. The suspension of human fibroblast cell line (NHDF) was placed in a 96-well plate at a density of 1 x 10^4 cells/well and incubated in DMEM containing 10%v/v FBS, 1%v/v penicillin/streptomycin and 0.1%v/v amphotericin B at 37°C in a CO_2 incubator for 24 hrs. The medium form NHDF well-plate was removed and then the cells washed by PBS. Cells were then treated with sterilized immersed medium from nanofiber samples at 37°C in a CO_2 incubator for 24 hrs. After treatment, they were washed with PBS before adding the mixture of 200 µL new serum-free medium and 50 µL XTT solution with an incubation time of 4 hrs. The cell viability was determined by measuring OD at 490 nm using a microplate reader. The value of each sample was compared with 100% viability of control and the percentage of cell viability was calculated following Eq.2.

In-vitro cell proliferation

Cell culture preparation. NHDF cell lines were cultured in a flask with DMEM medium supplemented with 10% v/v FBS, 1%v/v penicillin/streptomycin and 0.1%v/v amphotericin B incubated at 37 ºC under 5% CO_2 humidified atmosphere. The culture medium was refreshed every 3 days.

Sterilized core-shell electrospun nanofibers. The core-shell electrospun nanofibers were cut into 1.5 cm diameter discs and placed into a 24-well plate before being sterilized by ozone for 2 hrs, soaked in ethanol under UV light for 30 min and then washed with PBS solution.

Cell seeding. The sterilized core-shell electrospun nanofibers were immersed in DMEM containing 10% v/v FBS for 1 hr and then left for 1 hr in an incubator at 37°C. Then, human fibroblasts cell lines (7 x 10^4 cells/well) were seeded on each core-shell electrospun nanofiber sample for cell proliferation studies. Tissue culture polystyrene plates were used as the control group.

Cell proliferation by XTT assay. The proliferation of cells on the core-shell electrospun nanofibers was studied after 3 days of culture. Cultured nanofibers were transferred and placed into another 24-well plate with 200 µL of new serum-free medium to which 50 µL of XTT solution were added. This was left for 4 hrs in an incubator. Absorbance at 490 nm was measured with a microplate reader and cell viability was calculated based on Eq.2.

$$\text{Cell viability (\%)} = \frac{\text{OD}_S}{\text{OD}_C} \times 100 \qquad \text{Eq.2}$$

where OD_s is the absorbance of impregnated medium of nanofibers and OD_c is the absorbance of a control (incubated with culture medium without nanofibers or untreated cells).

3. Results and Discussion

Generally, when creating core-shell electrospun nanofiber fabrics, a hydrophobic core (with either hydrophilic or hydrophobic shell) allows a much simpler fabrication process. If the inside core utilizes organic solvents (e.g. chloroform and dimethyl sulfoxide), the formation of the core-fiber will be easier due to high solvent evaporation, compared to a hydrophilic core which normally uses water as solvent. This is the main reason why most of the research is designed either with a hydrophilic or hydrophobic shell but with predominately a hydrophobic core. Therefore, this causes limitations in the use of water-soluble bioactive agents, growth factors and other active agents.

In this work, the fibers have been designed to have a hydrophilic core with hydrophobic shell, therefore, the fabrication process presents a significant challenge. In contrast, however, this design enables the delivery of water-soluble agents from the core and the prevention of the premature release of these water-soluble agents by the shell. Therefore, the optimum conditions for fabrication of the core, shell and core-shell via co-axial electrospinning are importantly reported first. Subsequently, the new core-shell electrospun nanofibers [from water soluble (PVA/SS without crosslinker) and non-water soluble polymers (PLGA)] have been explored in terms of their antibacterial properties, *in vitro* toxicity and cell proliferation.

3.1 The Core (without shell): The effect of SS loading

PVA/SS nanofibers were fabricated using our green fabrication technique (only water and temperature of 70 °C was used) previously reported.[3] The concentration of PVA was fixed at 7 %w/v, while that of SS was changed between 0, 1, 2, 3 %w/v. The electrospinning parameters were used as shown in Fig.1a and the morphology of PVA and PVA/SS fibers are shown in Fig.1b. Smooth and uniform fibers were observed with 7 %w/v PVA with fiber diameter in the range of 200-450 nm. All 7 %w/v PVA samples incorporated with 1, 2, and 3 %w/v SS show fiber diameters in the range of 100-500 nm with beads. The formation of beads here is attributed to the low concentration of SS, especially at 1 %w/v SS, which results in a low degree of chain entanglement.[4,38] This means that beads are formed in electrospinning

when there are insufficient chain entanglements of the molecular chains, in this case the molecular chains of silk sericin.[39,40] Micro-droplets were found in the sample at 3%w/v SS, which were possibly caused by gelation of SS and then separation from PVA chains, and finally inhibited the production of homogeneous and smooth electrospun fibers. Therefore, 2 %w/v SS incorporated with 7 %w/v PVA was chosen to study further as the core component of the core-shell electrospun nanofibers. The electrospinning process parameters used were as follows; 0.02 mL/min flow rate, 25 kV and needle-to-collector distance of 15 cm.

a.

PVA (%w/v)	SS (%w/v)	Flow rate (mL/min)	Voltage (kV)	Distance (cm)	Note	Diameter nanofiber (nm)
7	0	0.02	25	15	Smooth nanofibers	200-400
7	1	0.02	25	15	Higher beads and micro-drops	<100
7	2	0.02	25	15	Smooth nanofibers and small beads	150-300
7	3	0.02	25	15	Smooth nanofibers and small beads	200-250

b.

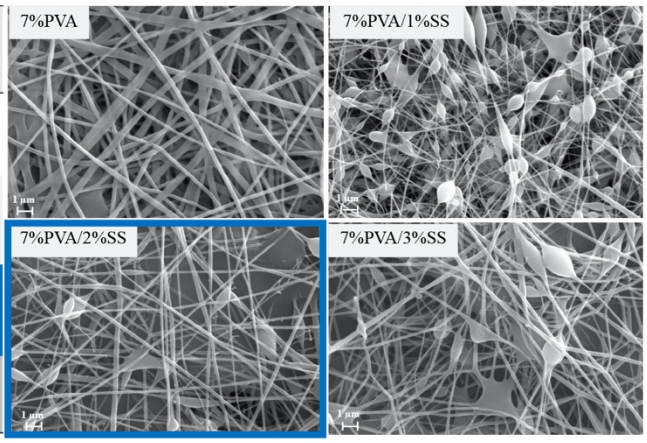

Figure 1. Electrospinning parameters of PVA/SS core-part (a) and corresponding SEM images of the electrospun fibers of PVA and PVA/SS at different SS concentrations (b).

3.2 The Shell (without core): The effect of PLGA concentration and molecular weight

PLGA was selected to fabricate the shell based on its ability to degrade in an aqueous environment and its use in numerous medical and pharmaceutical applications. Different concentrations of high molecular weight PLGA (HMW-PLGA, M_w = 108 kg.mol^{-1}) at 7 %w/v and 10 %w/v were used to fabricate fibers by electrospinning at the identified conditions (flow rate of 0.3 mL/h, voltage of 25 kV and distance from needle-to-collector of 15 cm).

Figures 2a and 2b show the morphologies of the fabricated fibers by SEM. At 7 %w/v HMW-PLGA (Fig.2a), nanofibers with beads are formed where fiber diameters were in the range of 500-700 nm. This is due to fewer chain entanglements caused by low polymer concentration, this is similar to effects seen with changes in solvent system of block copolymers where one of the polymer blocks retracts to reduce chain entanglements, resulting in the formation of beads.[9,10,41] Thus, HMW-PLGA at 10 %w/v (Fig.2b) presents smooth and uniform fibers with fiber diameters in the range of 700-1000 nm. Therefore, we chose to use 10 %w/v PLGA for further study as the shell. In addition, nanofibers were also fabricated from 10 %w/v

low molecular weight PLGA (LMW-PLGA, M_w = 20 kg.mol^{-1}) and the morphology is shown in Fig.2e (at day 0). Fibers of various diameters with the formation of both beads and micro-droplets can be observed. The morphology of the LMW-PLGA fibers was studied (dissolved in PBS solution at pH 7.4) and compared to HMW-PLGA fibers (Fig.2b) to assess the effect of molecular weight on the *in vitro* degradation of the shell material (without core).

As the shell layer serves as a barrier to prevent the premature release of the water-soluble agents from the core, the degradation of polymer shell is of vital importance to the process in the release of bioactive molecules from both the core and shell. Degradable polymers can undergo surface erosion or bulk erosion depending on the diffusion of water inside the matrix (linked to the matrix morphology and dimensions) and the degradation rate of the chemical linkages within the polymer.[42] However, the impact of these parameters on the degradation of the erosion mechanism is not fully clear yet. Conventionally, weight loss, swelling, molecular weight change and morphology are used to monitor the degradation of polymers. Therefore, the *in vitro* degradation of both the low and high molecular weight PLGA were studied and monitored by surface morphology and change in fiber diameter.

Figure 2c and 2d shows the average diameters and morphology of HMW-PLGA at different times of *in vitro* degradation test (at pH 7.4 and 37 °C), respectively. The results show that the diameters of HMW-PLGA fibers continuously increased with time. This is due to the swelling of PLGA fibers from the up-take of water in the polymer matrix. The weight loss of HMW-PLGA fibrous material reached 20% by day 63 (Fig.2c). In addition, the samples were left in solution for one year and the pH of the solution decreased from 7.4 to 5.4. This confirms that bulk erosion of PLGA can occur, where polymer chains degrade throughout the entire matrix. This possibly creates free carboxylic acid groups, which lead to a decrease of pH inside the swollen polymer matrix that accelerates the degree of ester hydrolysis.[43] Porous erosion zones were also observed on the HMW-PLGA surface (arrows in Fig.2d at day 63), which are caused by surface erosion. However, the degradation process of the HMW-PLGA is more likely to be bulk erosion than surface erosion, as the pH at 7.4 (neutral) slows down the degradation of the polymer matrix surface, as compared to the center. For LMW-PLGA fibers, broken fibers are clearly observed together with polymer swelling (Fig.2e). This is attributed to shorter PLGA chains cleaving faster when swelled and the osmotic pressure builds up inside the matrix due to the accumulation of degradation products, more than seen with longer chains of PLGA. In summary, HMW-PLGA was selected for study further as the shell component in in this work due to its ease of processability, stability in aqueous solution (important for

stability in fluid at the wound site) and degradability, which can be tailored for potential drug delivery systems in the future.

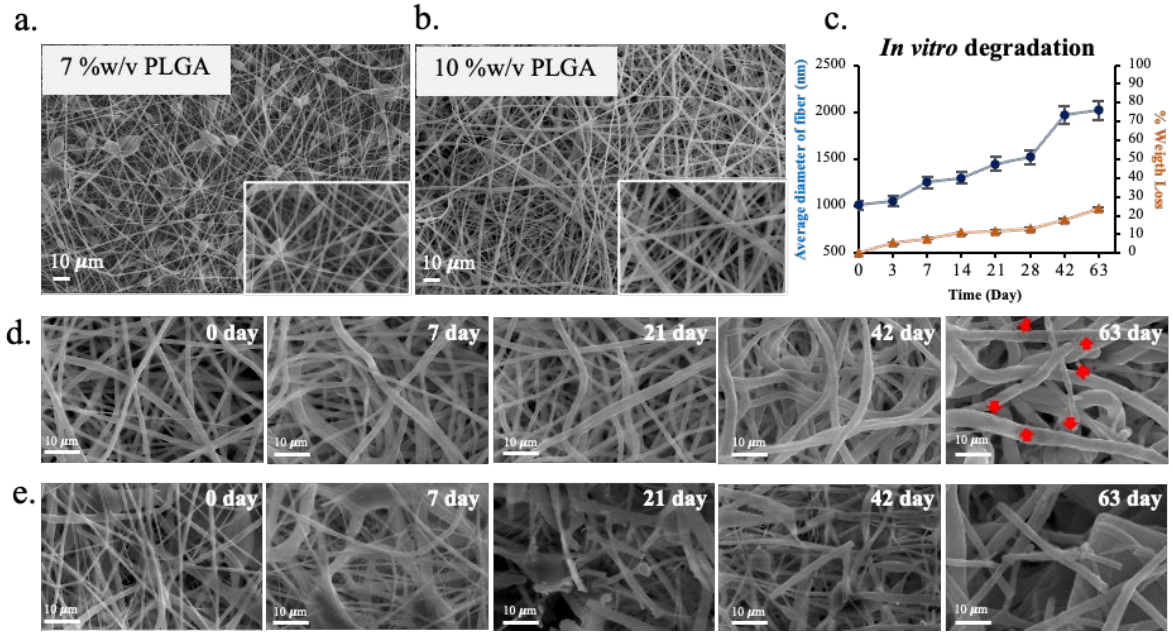

Figure 2. SEM images of high molecular weight PLGA at different concentrations for electrospinning of 7 %w/v (a) and 10 %w/v (b) at magnification of 500x (inset images of 2000x), the average diameters of 10 %w/v PLGA at different times of *in vitro degradation* at pH 7.4 (c), and SEM images of high molecular weight PLGA (d) and low molecular weight PLGA (e) at different time interval of submerging in PBS pH 7.4, at magnification of 2000, except at day 63 (at 5000x). Note: 0 day means the time before submerging in PBS pH7.4.

3.3 Core-Shell Electrospun Nanofibers (CSF): confirmation of morphology

In short, coaxial electrospinning is technically more complex than conventional single needle systems. Electrospun fibers are formed when the surface charge on the droplet induced by the electrical field is sufficiently high to overcome the surface tension of the polymer solution. As aforementioned, in the first component of this study, the optimal conditions for the core and the shell were elucidated individually. Consequently, the fabrication of core-shell electrospun nanofibers followed these identified conditions with 7 %w/v PVA and 2 %w/v SS and spinning flow rate of 0.2 mL/h (for the core), and 10 %w/v HMW-PLGA at 0.3 mL/h (for the shell). Both the core and shell used a spinning voltage of 25 kV and a tip-to-collector distance of 15 cm. The flow rate of PVA/SS for the core was changed from 1.2 mL/h (the condition used to fabricate core without shell) to 0.2 mL/h (for CSF), as there was slower

evaporation of water in the core layer (for CSF), when compared to its individual fabrication (core without shell).

Figure 3a, b and c show surface morphology of PVA/SS, HMW-PLGA and core-shell electrospun fibers of PVA/SS (core) - HMW-PLGA (shell) (CSFs), respectively. The porosity of the samples was determined by image analysis of the SEM images using ImageJ. The results gave % porosity of 45.14%, 26.95% and 31.03% for PVA/SS, PLGA and CSF, respectively. The CSFs were smooth and uniform with diameters in the range of 800-1300 nm, which are similar to the diameter of PLGA alone. The cross-section of the CSFs was also observed by SEM (Fig. 3d), revealing the discrete core and shell components. In addition, the successfully fabricated core-shell structures of PVA/SS-PLGA were observed by TEM, as shown in Fig.3e. This allows for the direct observation of core-shell structure, where the core PVA/SS appears black and the surrounding lighter grey area is the PLGA shell.

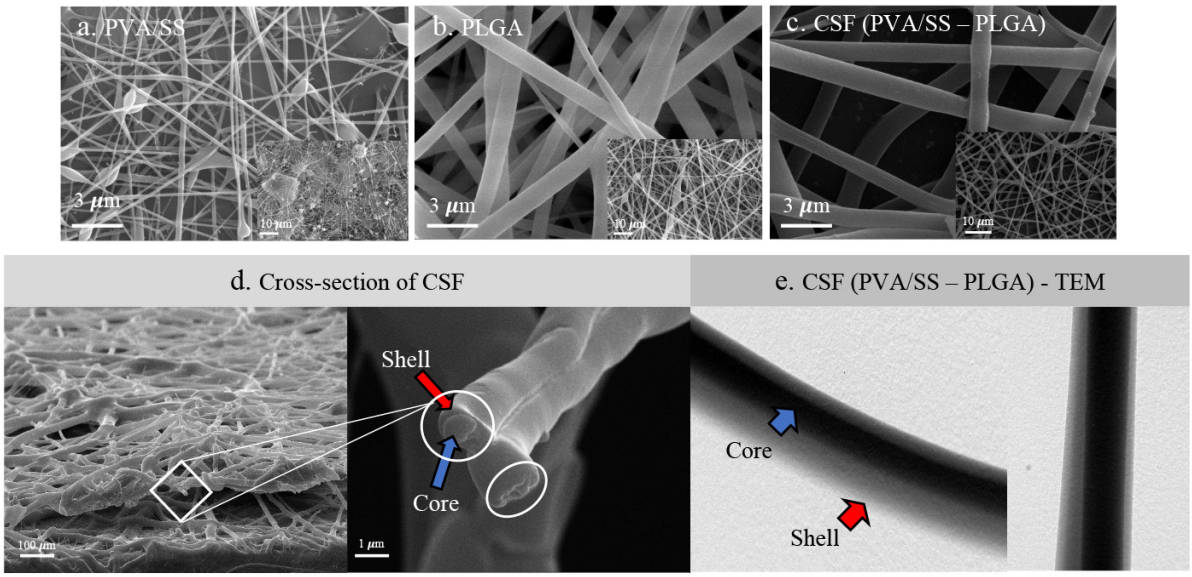

Figure 3. SEM images of electrospun nanofibers of; (a) 7 %w/v PVA / 2 %w/v SS, (b) 10 %w/v HMW-PLGA, (c) PVA/SS (core)-PLGA (shell) electrospun fibers (CSF), (d) cross-section of CSF and (e) TEM images of CSF.

Other techniques such as CA (Fig.4a), FT-IR (Fig.4b) and XRD (Fig.4c), were also used to confirm the achieved fabrication of the electrospun fibers in the form of core-shell structures. From Fig.4a, it is evident that PVA/SS electrospun fibers are hydrophilic (CA < 90^{o}), while PLGA and CSF fibers are hydrophobic (CA > 90^{o}). The CSF showed the same contact angle values as PLGA due to the fact that PLGA is the outer layer of the CSF. From Fig.4b, the surface functional groups of PVA/SS electrospun fibers show absorption bands at

3251 cm^{-1} (-OH stretching) of hydroxyl groups and 2906 cm^{-1} (-CH stretching) of PVA fibers and at 1645 and 1543 cm^{-1} of amide I and II from silk sericin (SS). PLGA electrospun fibers show absorption peaks at 2852 - 2922 cm^{-1} (-CH stretching), 1749 cm^{-1} (-C=O stretching vibration from ester bonds) and two peaks at 1084 and 1181 cm^{-1} (C-O stretching vibration from ester groups). Whereas the CSF produce FT-IR spectra with characteristic absorption bands identical to the PLGA electrospun fibers. In addition, the results of crystallinity by XRD (Fig.4c) show an amorphous broad peak (10-25^{o}) identical to the PLGA electrospun fibers.[44,45] Both results from FT-IR and XRD confirm that PLGA is the outer layer of the CSF.

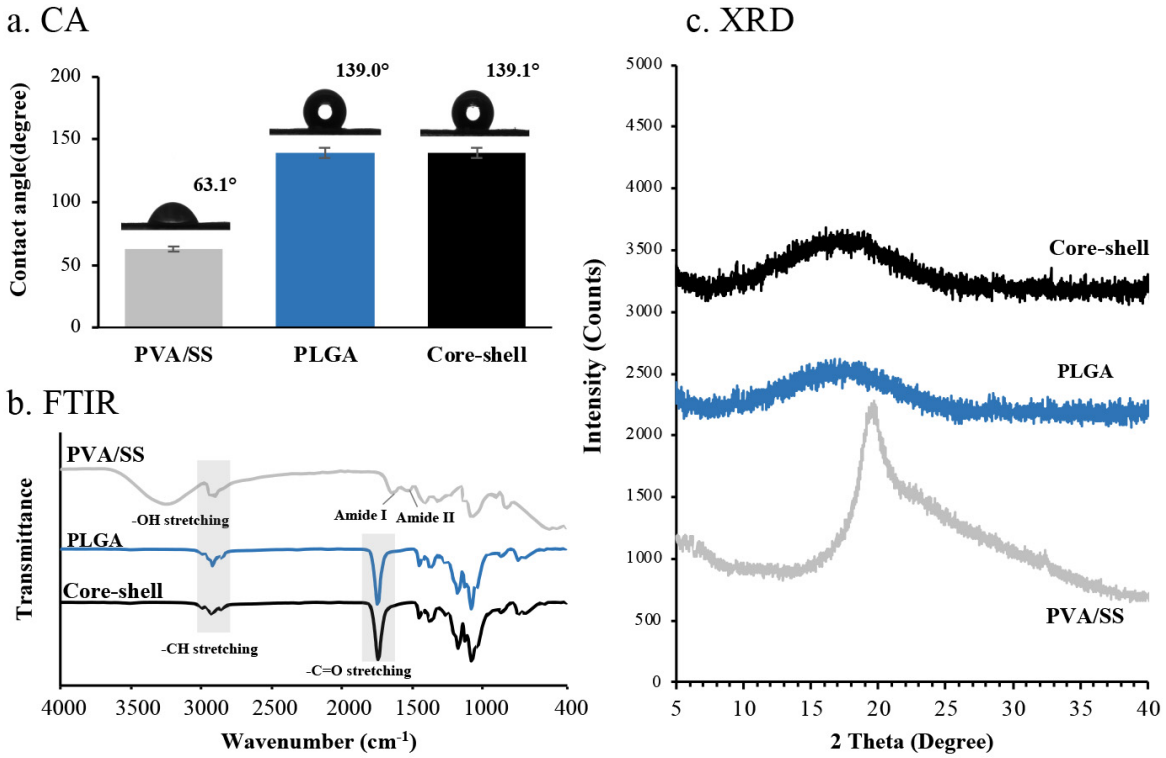

Figure 4. Surface properties of CSF: hydrophilicity by contact angle (a), chemical functionality by FT-IR (b), and crystallinity by XRD (c).

To further confirm the presence of the PVA/SS core within the PGLA shell, the CSF mats were immersed in chloroform (used to dissolve the hydrophobic PLGA shell, but not the hydrophilic PVA/SS core). Following immersion (3 hours) and removal of the remaining fibrous mat, the characteristic FT-IR peaks of PLGA were observed in the chloroform solution (see Fig. 5a. The remaining CSF mat was dried prior to FT-IR and SEM analysis, where the FT-IR spectrum shows characteristic peaks of PVA/SS (Fig. 5b) and the SEM image shows the fibrous morphology of PVA/SS (Fig. 5c). The results in Fig. 3, 4 and 5 show that the CSF

mats are composed of fibers with a PLGA shell and PVA/SS core, confirming successful fabrication of core-shell electrospun fibers of PVA/SS-PLGA.

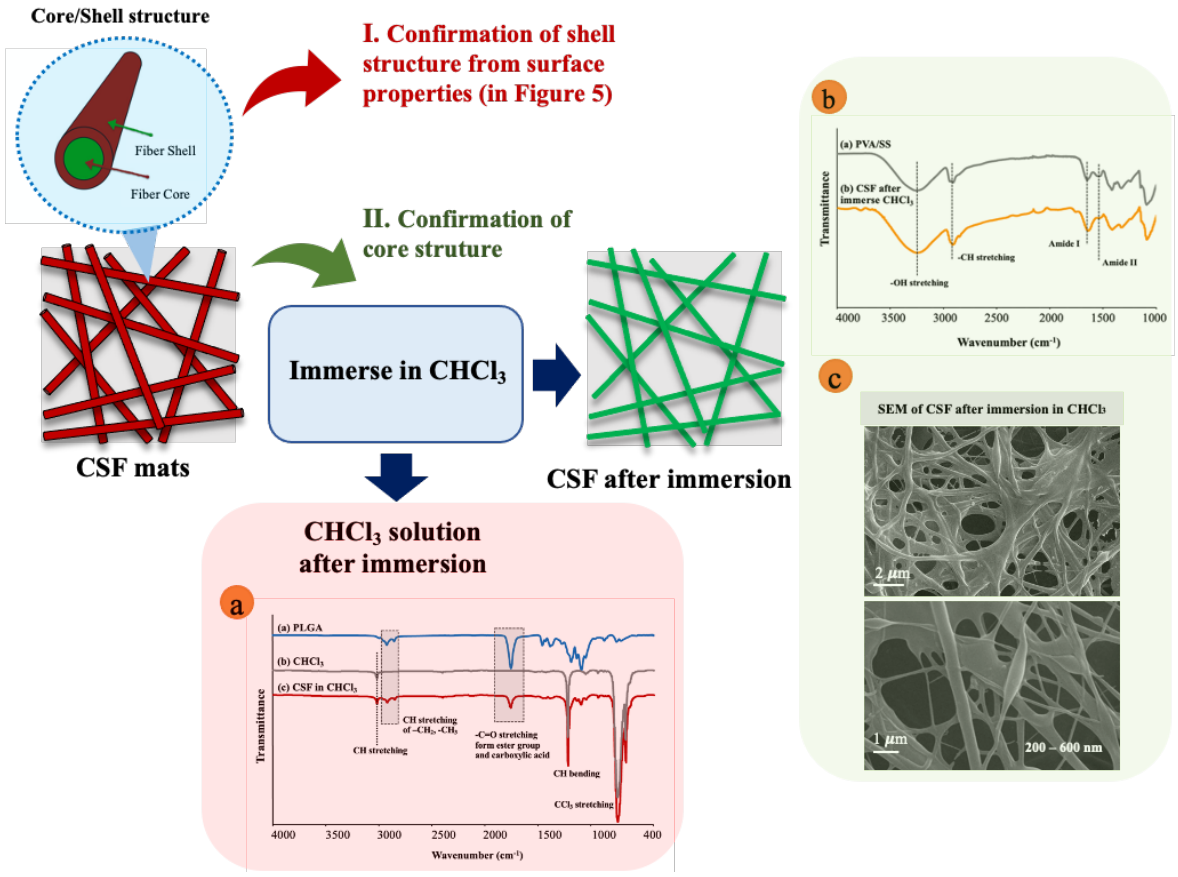

Figure 5. Schematic diagram of the method used to further confirm the core-shell morphology of the electrospun mats, showing the results following immersion of the CSF mats in chloroform: (a) FT-IR of the immersed chloroform solution (b); FT-IR of the CSF mats; and (c) SEM of CSF mats.

3.4 Antibacterial property of CSFs

One synthetic antimicrobial agent (silver nanoparticles, AgNPs) and one naturally derived extract (cinnamon essential oil, CEO) were chosen for deposition onto the CSFs in order to confer additional antimicrobial properties. The CSF/AgNP and CSF/CEO samples were studied for their antibacterial properties using Gram positive (*S. aureus*) and Gram negative (*E. coli*) bacteria via agar plate diffusion method. 6 mm diameter discs were prepared of a control (gentamycin), alongside CSF, CSF/AgNP and CSF/CEO (Fig.6a) and their inhibition zones were observed after incubation for 18 hrs at 37 °C (Fig.6b and 6c). Antibacterial activity against *E. coli* and *S. aureus* of CSF/AgNP gave inhibition zones of 6.50

± 0.14 mm and 6.56 ± 0.06 mm, respectively. The CSF/CEO samples showed clear inhibition zones of 9.60 ± 0.18 mm and 10.44 ± 0.06 mm, respectively. Indeed, our CSFs incorporated with either AgNP or CEO are able to inhibit the growth of these two types of bacteria.

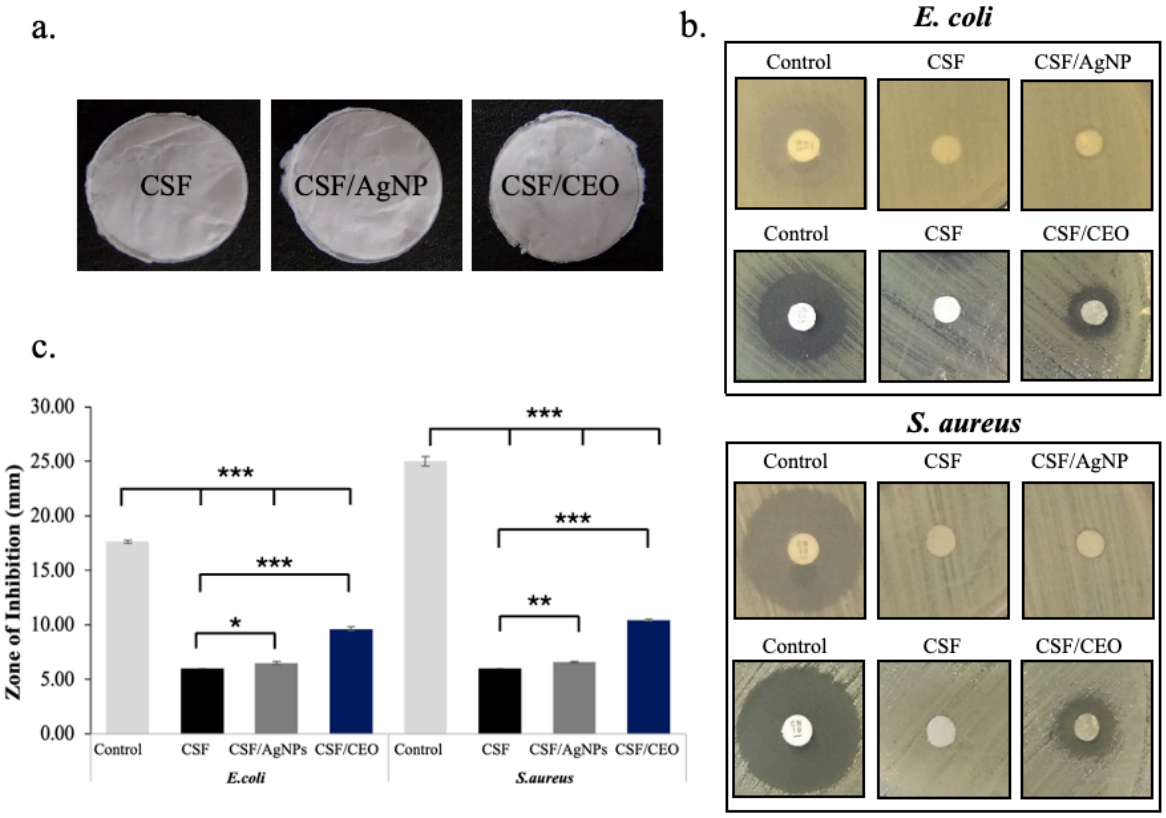

Figure 6. Photographs of core-shell electrospun fiber mats of CSF, CSF/AgNP and CSF/CEO (a) showing the zone of inhibition against Gram positive (*S. aureus*) and Gram negative (*E. coli*) bacteria via agar dish diffusion method (b) and zone of inhibition data compared to gentamycin as a control (c) * P <0.05, ** P<0.01 and *** P<0.001.

3.5 In vitro cytotoxicity and cell viability of CSF

Fig.7 shows the results of the *in vitro* cytotoxicity of CSF, CSF/AgNP and CSF/CEO examined using XTT assay and compared to a control. There is no difference in cell viabilities (for 24 hrs) between the control and all core-shell nanofibrous mats, which all exhibited high cell compatibility (>96 % cell viability) and no cytotoxicity. Morphological analysis reveals that NHDF cells could attach and proliferate on the surface of the fibers. In addition, we also examined the cell proliferation of CSF and CSF/AgNP using XTT assay and observed cell viability (%) at day 1 and day 3 with the results shown in Fig.8. For all CSF samples, NHDF cells exhibit a good tolerance to the nanofibrous fabrics, after 24 hours of culture, the cell viability of all samples was more than 85%, which demonstrates their nontoxicity. Although

time dependent variabilities were observed, with a reduction of cell viability detected in the CSF/AgNP nanofibrous scaffolds and an increase with the CSF nanofibrous scaffolds (from 98.7% to 144.5%). The greater cell viability seen with the CSF scaffold (144.5%) is due to the extra space present within 3D structures of scaffolds (acting as ECM) when compared to the 2D control plate.[46] The decrease of cell viability of CSF/AgNP after 72 hrs of incubation might be due to the fact that the metal nanoparticles can trigger several toxic side-effects by inducing cell oxidative stress, apoptosis and mitochondrial dysfunction, as well as membrane and DNA damage.[47-49]

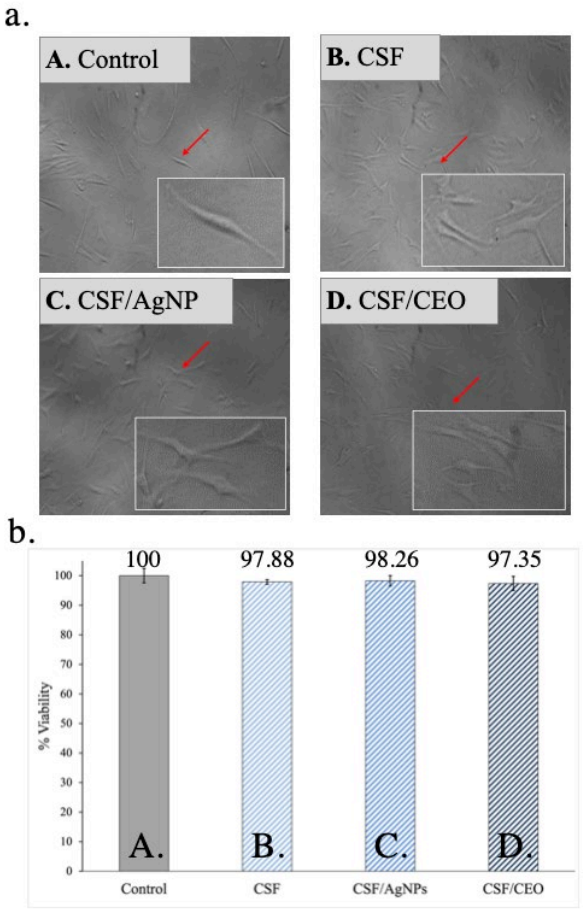

Figure 7. Indirect *in vitro* cytotoxicity of core-shell electrospun nanofibrous mats (CSF, CSF-AgNP, CSF/CEO) after 24 hrs of XTT assay: (a) optical microscope of cells on well-plates of immersed medium from different nanofiber samples and (b) cell viability (%) of NHDF (n = 9).

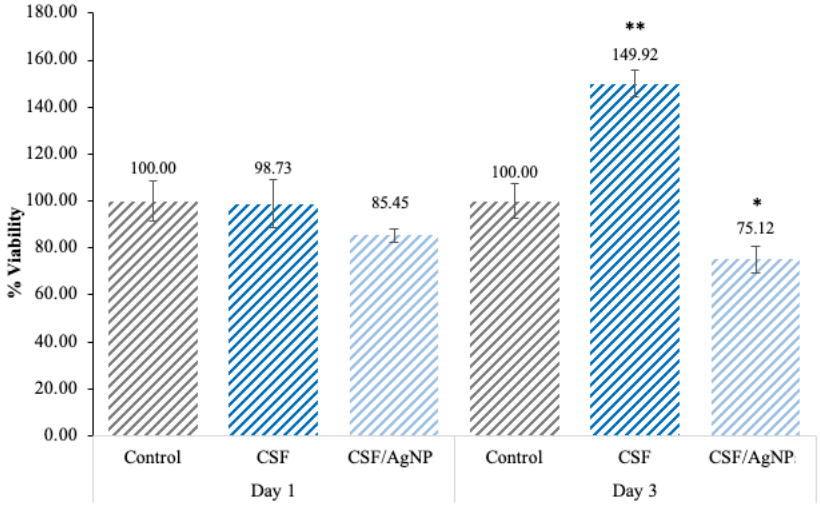

Figure 8. Viability of NHDF cells from XTT assay on the different types of core-shell electrospun nanofibrous mats (CSF and CSF/AgNP) after 1 day and 3 days of culture (n = 3). * P <0.05, ** P<0.01

4. Conclusions

Novel core-shell nanofibrous scaffolds of PVA/SS (hydrophilic core) and PLGA (hydrophobic shell) were successfully fabricated *via* coaxial electrospinning. Operating conditions were studied and suitable parameters identified to obtain optimal fibrous morphology; 7 %w/v PVA and 2 %w/v SS and spinning flow rate of 0.2 mL/h (for the core), and 10 %w/v HMW-PLGA at 0.3 mL/h (for the shell), a spinning voltage of 25 kV and a tip-to-collector distance of 15 cm. The core-shell nanofibers (CSFs) were smooth and uniform with diameters in the range of 800 - 1300 nm. The results from SEM, FT-IR, CA and XRD confirmed successful fabrication of core-shell electrospun fibers of PVA/SS-PLGA. In addition, these CSFs show potential to deliver antibacterial protection, and NHDF cell adhesion and proliferation. This smart multifunctional core-shell electrospun nanofibrous fabric has demonstrated its potential to be used as an innovative biomedical system that can: (i) incorporate additional bioactive agents, growth factors or other agents embedded into the core; (ii) contain antibacterial agents within the shell; and (iii) function as an extracellular matrix to enable cells to migrate and grow. Future work will focus on developing these systems further for use in wound protection and smart repair.

Acknowledgements

This work was funded by the Biodiversity-Based Economy Development Office (Public Organization) – Bioplastics section (2017), Thailand [grant number 486754] and has received funding from the European Union's Horizon 2020 research and innovation programme under the Marie Sklodowska-Curie grant agreement No 871650. This research was also partially supported by the Program Management Unit for Human Resources & Institutional Development, Research and Innovation, Office of National Higher Education Science Research and Innovation Policy Council (NXPO), Thailand [Grant Number B16F640001]) and Center of Excellence in Materials Science and Technology, Chiang Mai University. Also, thanks to the Science Lab Centre, Faculty of Science, Naresuan University for supporting XRD, DSC, CA, SEM and FTIR measurements.

Data Availability

The raw/processed data required to reproduce these findings cannot be shared at this time as the data also forms part of an ongoing study.

References

1. Badylak SF, *Semin Cell Dev Biol* **13(5):** 377-383 (2002) .
2. Pham QP, Sharma U, et al., *Tissue Eng* **12:** 1197-1211 (2006).
3. Kumkun P, Tuancharoensri N, Ross GM, Mahasaranon S, Jongjitwimol J, Topham PD and Ross S, *Polym Inter* **68:** 1903–1913 (2019).
4. Tuancharoensri N, Ross GM, Mahasaranon S, Topham PD and Ross S, *Polym Inter* **66(11):** 1463-1472 (2017).
5. Chen L, Wang S, Yu Q, Topham PD, Chen C and Wang L, *Soft Matter* **15(12):** 2490-2510 (2019).
6. Abrigo M, McArthur S and Kingshott P, *Macromol Biosci* **14:** 772–792 (2014).
7. Li W, Yu Q, Yao H, Zhu Y, Topham PD, Yue K, Ren L and Wang L, *Acta Biomaterialia* **92:** 60-70 (2019).
8. Wang L, Wang M, Topham PD, Huang Y, *RSC Advances* **2(6):** 2433-2438 (2012).
9. Agarwal V, Ho D, Ho D, Galabura Y, et al., ACS Appl Mater Interfaces 8(7): 4934-4939 (2016)
10. Majumder S, Matin MA, Sharif A and Arafat MT, J Polym Res 27:381 (2020)
11. Menini R and Farzaneh M, Polym Int 57(1): 77-84 (2008)

12. Ross S, Yooyod M, Limpeanchob N, Mahasaranon S, Suphrom N and Ross GM, *eXpress Polym Lett* **11(9):** 719-730 (2017).

13. Ross S, Topham PD and Tighe BJ, *Polym Inter* **66:** 44-51 (2013).

14. Ross S, Mahasaranon S and Ross GM, *J Appl Polym Sci* **132(4):** 41780(1-8) (2015).

15. Ross GM, Ross S and Tighe BJ, Chapter 23-Bioplastics: New Routes, New Products, in *Brydson's Plastics Materials* 8th ed., ed by Gillert M. Oxford: Butterworth Heinemann, pp 631-652 (2007).

16. Alharbi HF, Lungman M, Khalil KA, Elnakady YA, Abd-Elkader OH, Rady AM, Alharthi NH and Karim MR, *Eur Polym J* **98:** 483-491(2018).

17. Nguyen TTT, Chung OH and Park JS, *Carbohyd Polym* **86:** 1799-1806 (2011).

18. Abdal-hay A, Hussein KH, Casettari L, Khalil KA and Hamdy AS, *Mater Sci Eng C* **60:** 143-150 (2016).

19. Tang Y, Chen L, Zhao K, Wu Z, Wang Y and Tan Q, *Comps Sci Technol* **125:** 100-107 (2016).

20. Shahverdi S, Hajimiri M, Esfandiari MA, Larijani B, Atyabi F, Rajabiani A, Dehpour AR, Gharehaghaji AA and Dinarvan R, *Inter J Pharm* **473:** 345-355 (2014).

21. Guimaraes PPG, Oliveria MF, Gomes ADM, Gontijo SML, Cortes ME, Campos PP, Viana CTR, Andrade SP, Sinisterra RD, *Colloids Surf B* **136:** 248-255 (2015).

22. He P, Zhong Q, Ge Y, Guo Z, Tian J, Zhou Y, Ding S, Li H and Zhou C, *Mater Sci Eng C* **90:** 549-556 (2018).

23. Mehrasa M, Asadollahi MA, Ghaedi K, Salehi H and Arpanaei A, *Int J Biol Macromol* **79:** 687-695 (2015).

24. Ershuai Z, Chuanshun Z, Jun Y, Hong S, Xiaomin Z, Suhua L, Yonglan W, Lu S and Fanglian Y, *Mater Sci Eng C* **58:** 278-285 (2016).

25. Surucu S and Sasmazel HT, *Int J Biol Macromol* **92:** 321-328 (2016).

26. Sedghi R and Shaabani A, *Polymer* **101:** 151-157 (2016).

27. Yan S, Li X, Dai J, Wang Y, Wang B, Lu Y, Shi J, Huang P, Gong J and Yao Y, *Mater Sci. Eng C* **79:** 436-444 (2017).

28. Demir MM, Ugur G, Gulgun MA and Menceloglu YZ, *Macromol Chem & Phys* **209(5):** 508-515 (2008)

29. Agarwal V, Wood FM, Fear MW and Iyer KS, *Aust J Chem* **70(3):** A-F (2016).

30. Oktay B, Demir S and Kayaman-Apohan N, *Mater Sci Eng C Mater Biol Appl* **50:** 386-393 (2015).

31. Aramwit P, Siritientong T, Kanokpanont S and Srichana T, *Inter J Biol Macromol* **47:** 668-675 (2010).

32. Gilotra S, Chouhan D, Bhardwaj N, Nandi SK and Mandal BB, *Mater Sci Eng C* **90:** 420-432 (2018).

33. Shahverdi S, Hajimiri M, Esfandiari MA, Larijani B, Atyabi F, Rajabiani A, Dehpour AR, Gharehaghaji AA and Dinarvand R, *Int J Pharm* **473:** 345-355 (2014).

34. Nguyen TTT, Chung OH and Par JS, *Carbohyd Polym* **86:** 1799-1806 (2011)

35. Yan E, Jiang J, Ren X, Gao J, Zhang X, Li S, Chen S and Li Y, *Mat Lett* **291:** 129516-129519 (2021)

36. Alharbi HF, Lugman M, Khalil KA, Elnakady YA, et al., *Europ Polym J* **98:** 483-491 (2018)

37. Yooyod M, Ross GM, Limpeanchob N, Suphrom N, Mahasaranon S and Ross S, *Eur Polym J* **81:** 43-52 (2016).

38. Yu JH, Fridrikh SV and Rutledge GC, *Polymer* **47:** 4789–4797 (2006).

39. Agarwal S, Greiner A and Wendorff JH, *Prog Polym Sci* **38(6):** 963-991

40. Arinstein A and Zussman, *J Polym Sci B: Polym Phy* **49(10):** 691-707

41. L. Wang L, Topham PD, Mykhaylyk OO, Yu H, Ryan AJ, Fairclough JPA and Bras W, *Macromol Rapid Commun* **36(15):** 1437-1443 (2015).

42. Burkersrodaa F.von, Schedlb L and Gopferich A, *Biomaterials* **23:** 4221–4231 (2002).

43. Sykes PM, A guidebook to mechanism in organic chemistry, 4th ed. London: Longman, (1975).

44. Hu H, Jian W, Lan F, Zeng X, Ma S, Wu Y and Gu Z, *RSC Advanc* **3(3):** 879-886 (2012)

45. Fang Y, Liu F, Xu L, Wang P and He J, *Polymers* **10(481):** 1-15 (2018)

46. Sung KE, Su X, Berthier E, Pehlke C, Friedl A and Beebe DJ, *PLOS ONE* **8(10) e76373:** 1-13 (2013).

47. Tak YK, Pal S, Naoghare PK, Rangasamy S and Song JM, *Sci Rep* **51(6908):**1-11 (2015).

48. Filon FL, Bello D, Cherrie JW, Sleeuwenhoek A, Spaan S and Brouwer DH, *Int J Hyg Environ Health* **219:** 536–544 (2016).

49. Wang M, Lai X, Shao L and Li L, *Int J Nanomed* **13:** 4445-4459 (2018).

Graphical Abstract

Smart multifunctional core-shell electrospun nanofibrous fabrics of poly(vinyl alcohol)/silk sericin (core) and poly(lactide-*co*-glycolide) (shell)

Nantaprapa Tuancharoensri[1], Gareth Ross[1,2], Winita Punyodom[3,4], Sararat Mahasaranon[1,2], Jirapas Jongjitwimol[5], Paul D Topham[6], Sukunya Ross[1,2,*]

Corresponding author, e-mail address: sukunyaj@nu.ac.th